

## Satellite-derived shallow wetland bathymetry using different classification algorithms and datasets

Adalet Dervisoglu<sup>a,\*</sup>, Nur Yagmur<sup>a</sup>, Burhan Baha Bilgilioglu<sup>a,b</sup>

<sup>a</sup>Department of Geomatics Engineering, Civil Engineering Faculty, Istanbul Technical University, Istanbul, Turkey, emails: [adervisoglu@itu.edu.tr](mailto:adervisoglu@itu.edu.tr) (A. Dervisoglu), [yagmurn@itu.edu.tr](mailto:yagmurn@itu.edu.tr) (N. Yagmur), [bahabilgilioglu@gumushane.edu.tr](mailto:bahabilgilioglu@gumushane.edu.tr) (B.B. Bilgilioglu)

<sup>b</sup>Department of Geomatics Engineering, Engineering and Natural Science Faculty, Gumushane University, Gumushane, Turkey

Received 27 April 2021; Accepted 2 October 2021

---

### ABSTRACT

Remote sensing (RS) effectively identifies, analyzes, and monitors wetlands. In addition to these two-dimensional studies, RS is used with several techniques in determining shallow water depths. The primary purpose of this study is to obtain shallow wetland bathymetry utilizing spectral reflections obtained at different water depths by field study and satellite images. Machine learning (ML) algorithms, which are widely used in remote sensing, are used in this study. Four algorithms were selected as random forest (RF), support vector machine (SVM), Neural Networks (NN), and Maximum Likelihood Classification (MLC). Since machine learning algorithms use training samples/datasets, the classification accuracy is directly related to selecting these data. The effect of pixel counts on classification was investigated by using two different training data set also. Duden (Kulu) Lake, which is a shallow wetland, was chosen as the study area. The Iterative Self-Organizing Data Analysis Technique (ISODATA) classification algorithm divided into as many clusters as possible was applied on Sentinel-2 multispectral images. All classes were redefined using measured spectral signatures and were created a bathymetric map. This map was used as reference data in creating training sets and the accuracy assessment of ML algorithms. When the water surface areas obtained from algorithms were compared with the bathymetric map and Normalized Difference Water Index, the best result was obtained with RF. According to the accuracy assessment results, it was seen that the number of training data affects the accuracy, and the best results were obtained with SVM and RF algorithms with training data containing more pixels (overall accuracy 93.87% and 92.64, kappa 0.89 and 0.87, respectively).

*Keywords:* Wetland; Remote sensing; Satellite-derived bathymetry; Machine learning; Maximum likelihood classification; Support vector machine; Random forest; Neural networks

---

### 1. Introduction

Wetlands provide breeding, growing, and feeding opportunities to many fish and wildlife species and are shallow waters considered the bridge between terrestrial and water systems [1]. In addition, wetlands and lakes play a crucial role in the Earth's surface system, such as the atmosphere, hydrosphere, etc., and are affected by environmental changes and human activities [2]. With the understanding of the importance of wetlands in recent years, efforts have

been made to protect these areas. The first step in protecting wetlands is to map these areas and then regularly monitor them. However, because of the wildlife and structure of wetlands, accessing them is often complicated and complex; mapping and monitoring wetlands via remote sensing (RS) is the optimal solution [3].

RS is defined as the acquisition and measurement of information about certain properties of phenomena, objects, or materials by a recording device, not in physical contact with the features under surveillance [4]. Electromagnetic

---

\* Corresponding author.

radiation (EMR) is described as all energy that moves with the velocity of light in a harmonic wave pattern. When EMR comes into contact with any object or material such as water, buildings, or atmospheric gases, it can be absorbed, reflected, scattered, or emitted. RS is principally based on detecting and recording reflected and emitted EMR. What essentially makes remote sensing possible is that each object or material has certain emission and/or reflective properties known as its spectral signature or profile, which distinguish it from other objects and materials. Satellite, aerial or ground-based RS sensors are tuned to collect this “spectral” data [4].

RS-based methods make it possible to generate accurate maps of shallow water areas by coupling remote sensing data with ground-based measurements while reducing or eliminating the time-consuming ground-based measurements [5]. There are numerous methods such as spectral indices, thresholding, and classification for detecting surface water areas with remotely sensed multi-band images. The reflectance of shallow water is dependent on the bottom type of the water, but using the ratio of spectral reflectances decreases the sensibility of bottom albedo [6]. Several empirical and semi-analytical methods are based on the band ratio models and apply models with the assumption of vertically homogeneous water columns [7]. These models are valid if it is considered that total reflectance of water-related to turbidity and water depth [8]. However, very shallow and transparent water bottoms are the exception in these models [9]. Classification maps are the main product of remote sensing image processing and pixel-based classification uses spectral reflectivity of features. Many pixel-based classification algorithms have been used to map land use land cover (LULC) and their changes from remotely sensed data. Unsupervised and supervised classification methods are widely used for mapping wetlands using different remote sensing data [10]. Unsupervised classification and cluster labeling is the dominant method for large area LULC mapping, and unsupervised classification involves a considerable dataset, and the algorithm has to cluster that dataset into various classes [11]. The most commonly used unsupervised method is the Iterative Self-Organizing Data Analysis Technique (ISODATA), which was developed by Ball and Hall [12]. It is a mathematical algorithm and stated that it gives better results in many studies [13]. ISODATA algorithm allows for a different number of clusters and calculates the class means iteratively using minimum distance [14]. It is widely used for LULC classification [15]. In the case of supervised machine learning, image classification methods use labeled information (training data) about class membership of single pixels (labeled by expert users) to build a model able to generalize to the whole image [16]. The most commonly used methods are random forest (RF), support vector machines (SVM), Neural Networks (NN), and Maximum Likelihood Classification (MLC).

Machine learning (ML) algorithms have come out as more accurate and efficient alternatives to conventional parametric algorithms in the last decades. Machine learning has been successfully applied in remote sensing for wetland classification [16]. Tian et al. [17] applied the RF classification method to detect the wetland land cover.

Amani et al. [18] compared the five different ML classifiers (K-nearest neighbor, MLC, SVM, classification and regression trees, and RF) in terms of performance in the wetland classification, and the results showed that the overall accuracies of classifications were nearly similar, except RF classifier. Yagmur et al. [19] used the SVM algorithm to classify shallow wetlands according to the depth of the water using spectral bands of satellite images and spectral water indices. Unsupervised classification can also be used to understand similar classes in the satellite images and prepare reference data, including training and validation in supervised classification. Wagle et al. [20] applied the unsupervised classification to prepare reference data and evaluate the performance of ensemble learning methods, RF and XGBoost, for LULC classification.

Bathymetry quantifies depths to study the topography of water bodies, and bathymetric mapping is the process of making bathymetric maps based upon the depth data. Traditionally, bathymetry is produced by interpolating depth data collected by echo sounders, and the digital terrain/bathymetric models are created [21]. Compared with traditional, the RS method is faster and more applicable to various environments, including shallow coastal waters and clear rivers which cannot be reachable for in-situ measurements. Bathymetry can be estimated using several RS techniques, each having its depth detection capability, accuracy, strengths/advantages, drawbacks, and best application environment [22]. Imagery-derived bathymetry is cost-effective and provides extensive area analysis. Besides, it is produced and has a lower accuracy than LIDAR or echo sounders [23].

Depth information obtained by analyzing satellite images is called satellite-derived bathymetry (SDB). There are two approaches to extracting water depth from satellite imagery: physics-based inversion algorithms and in-situ measurements to show reflectance to depth relationship [6]. This study applied an approach to classify shallow water areas using a spectroradiometer and depth data measurements. Detecting surface water using optical remote sensing is based on the difference between the spectral reflectance of land and water. Water absorbs most of the near-infrared (NIR) energy and mid-infrared (MIR) wavelengths; however, vegetation, soil, and impervious surfaces have a higher reflectance in these wavelengths. Therefore, in a multi-spectral image, water appears a darker tone in the infrared (IR) bands and can be easily differentiated from dry land surfaces [24].

There are a few studies for deriving bathymetry of water bodies using optical satellite images. Kerr and Purkis [25] proposed a new algorithm for deriving bathymetry using multi-resolution satellite data, bottom reflectance, and water depth in coral reef landscapes. Ai et al. [26] retrieved water depth using high-resolution satellite images with a deep learning algorithm in a shallow marine area.

The study's primary purpose is to present an approach to produce the bathymetry of shallow wetlands, which do not have bathymetry and could not be generated due to ground conditions, by utilizing the spectral reflections of water at different depths. Besides, the potential of ML algorithms in the determination of satellite-derived shallow wetland bathymetry based on spectral measurements was

investigated using Sentinel-2 satellite images. Unsupervised ISODATA classification was made with 300 clusters; spectral reflections in each cluster were examined one by one and assigned to four water groups and non-water. This classification was used as reference data to create two different training datasets. These training datasets were produced according to the different pixels, like greater than 100 or not in each training polygon. The study used training datasets for classification with RF, SVM, MLC, and NN algorithms. Accuracy assessment of the eight classified maps was made based on the generated reference bathymetric map. Additionally, a class-based areal comparison of results was investigated with the reference data.

## 2. Study area

Duden Lake is a tectonic lake in the middle of Turkey, in the Konya Closed Basin, within the provincial borders of Ankara at an altitude of 950 m above sea level (Fig. 1). There are freshwater ecosystems, saltwater ecosystems, and associated flat steppes in the region and a small freshwater lake in the south of the lake. The reeds on the shore of the freshwater lake are essential breeding grounds for waterfowl and are the most critical growth point for the worldwide endangered white-headed duck. In addition, the lake is a crucial accommodation point during the migration periods of shorebirds and is a closed, shallow wetland with 185 bird species, primarily flamingos. For these reasons, it was declared a qualified natural site in 2020 [27].

The sources feeding the lake are Kulu Creek, groundwater, and precipitation. The most critical threat to the lake is the drop in the water level of the area. Excessive

groundwater use due to wrong product pattern, which is the general problem in Konya Closed Basin, and unplanned interventions on water resources brought Kulu to the point of extinction, like other lakes in the basin [30].

Since the water coming from Kulu Creek is used in the agricultural areas around the lake from the spring months, the only source that feeds the site is precipitation most of the time. When the precipitation and evaporation data of Kulu Meteorology Station, which is approximately 6 km away from the lake, are examined, it is seen that the average amount of evaporation is exceptionally high compared to the average amount of precipitation (Fig. 2). For example, while the average precipitation in July is 12.5 mm, evaporation is 260.8 mm, and the amount of evaporation is approximately 20.9 times the precipitation amount. For this reason, water is seen in the lake during the months with the highest precipitation (winter and spring months). Water almost disappears in the region during the summer months and September, as seen in Fig. 3. As of October, with the onset of precipitation and the ending of agricultural water use, water begins to collect in the lake.

## 3. Data used and methodology

### 3.1. Data used

#### 3.1.1. Sentinel-2 data

The Sentinel satellites were designed by the European Commission's Copernicus program to deliver the wealth of data and imagery for Europe. The Sentinel-2 has provided freely available data of Earth's land surface since 2015 and has 13 spectral bands whose spatial resolutions differ

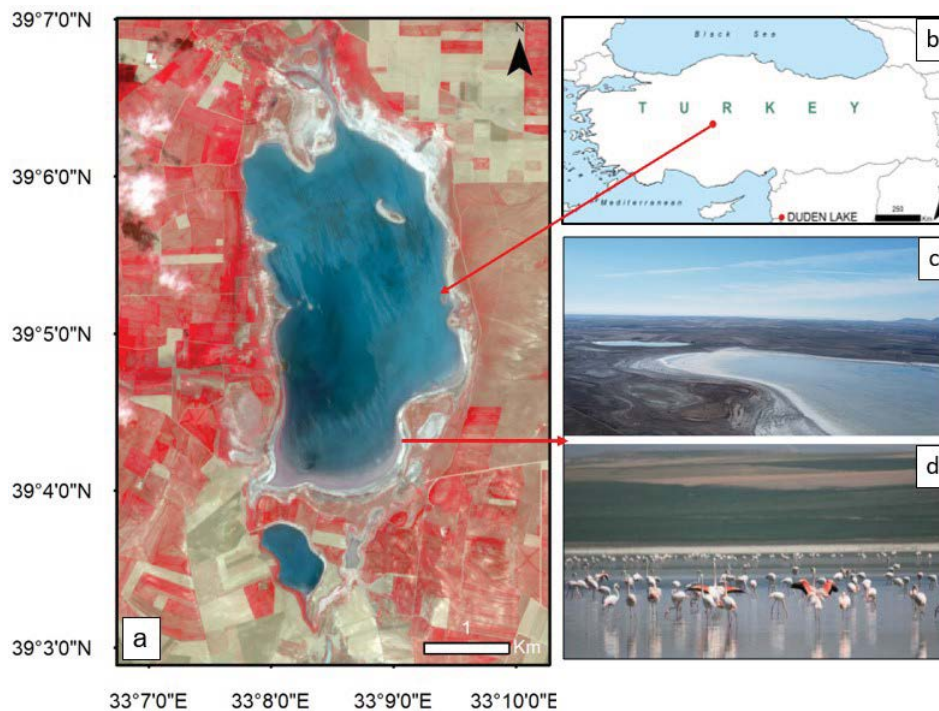


Fig. 1. (a) Duden Lake (false color combination of Sentinel-2 image), (b) Location in the map of Turkey (c and d) views from Duden Lake [28,29].

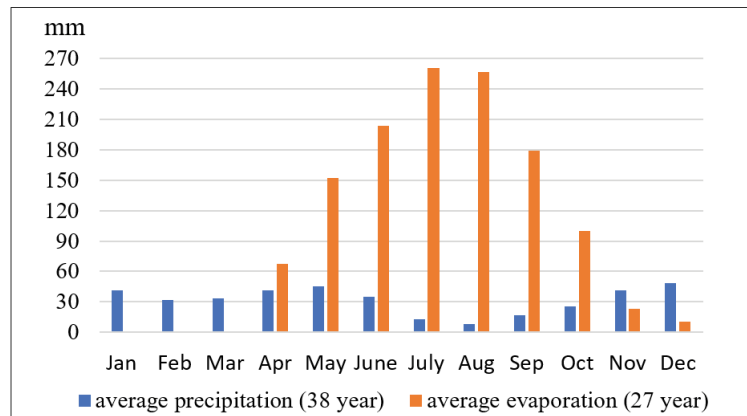


Fig. 2. Kulu meteorological station average precipitation and evaporation data.



Fig. 3. Duden Lake on different dates (Sentinel-2 MSI).

Table 1  
Sentinel-2 satellite image details [25]

Resolution	Sentinel-2 MSI
Spatial (m)	B1: Coastal aerosol, B9: Water vapor, B10: SWIR Cirrus = 60 m B2: Blue, B3: Green, B4: Red, B8: NIR = 10 m B5, B6, B7, B8A: Vegetation Red Edge, B11, B12: SWIR 1–2 = 20 m
Radiometric (bit)	12
Temporal (d)	5
Spectral (central wavelength) (µm)	B1: 0.443, B2: 0.490, B3: 0.560, B4: 0.665, B5: 0.705, B6: 0.740, B7: 0.783, B8: 0.842, B8A: 0.865, B9: 0.945, B10: 1.375, B11: 1.610 µm, B12: 2.190

from 10 to 60 m. Sentinel-2 Level-2A data is an orthoimage Bottom-of-Atmosphere (BOA) radiometrically and geometrically corrected reflectance product images. A field study was carried out on the same day and at about the same time as the satellite image date, and water reflectance values were measured. Sentinel-2 multispectral image (MSI) Level 2 image information dated April 27, 2019, used is given in Table 1 [31].

### 3.1.2. Spectral reflectances

Water’s spectral reflectance at different water depths was measured 20 times at 5–10 points (water1 = 10, water2 = 10, water3 = 8, water4 = 5) for each depth with the FieldSpec handheld spectroradiometer covering the 325 to 1,075 nm range. Measured water depths with an aluminum leveling rod are ≥30 cm, 15–20 cm, 5–10 cm, ≤5 cm. The spectral

signatures of water and wet soil measured by spectroradiometer are given as an example in Fig. 4.

Since the spectroradiometer measures between 325 to 1,075 nm, spectral bands of the satellite image were selected according to this interval. Spectroradiometer measurements were done simultaneously with the acquisition of the satellite image. That is why surface reflectance satellite images were used, and nine bands (from Band 1 to Band 8A) were selected for the classification process. Also, it is important to use multiple bands for eliminating the problem of a variety of in-water optical properties [32].

According to Mobley [33], the water depth and spectral reflectance are directly related to each other and water depth can be determined via their relationship. Sentinel-2 MSI band center points were marked on each spectral reflection graph obtained from spectroradiometer measurements and averaged. The averages of these spectral reflection curves measured by spectroradiometer at four different water depths and wet ground and resampled to Sentinel-2 are given in Fig. 5a. The reflections of the four water classes taken on the Sentinel-2 MSI image are presented in Fig. 5b.

The area where spectroradiometers (spectrometers) and depth measurements were made at different water depths are shown on the Sentinel-2 true color combination in

Fig. 6 with red circles. Swampy areas surround the lake, so measurements were made in only the non-swampy area.

### 3.2. Methodology

As the first process, the ISODATA (Recursive Self-Organizing DATA) classification was applied. The 2,050 ha lake and its surroundings were divided into 300 clusters and the spectral reflections of each class were compared with the measured spectra. The clusters were collected in five classes: four water classes and non-water classes, and a bathymetric map was created as a reference map. The training data required for the implementation of ML algorithms was taken from this thematic map for each class. A sufficient number of training samples are critical for image classifications [34–36]. Furthermore, since machine learning algorithms construct a mathematical model based on training data, sample data selection is significant. Supervised classifications were made to show the classification performance of each ML algorithm with two approaches: training polygons contained less than equal 100 pixels (dataset1) and more than 100 pixels (dataset2).

In this study, Duden Lake was evaluated with different pixel-based classification algorithms. Four supervised ML

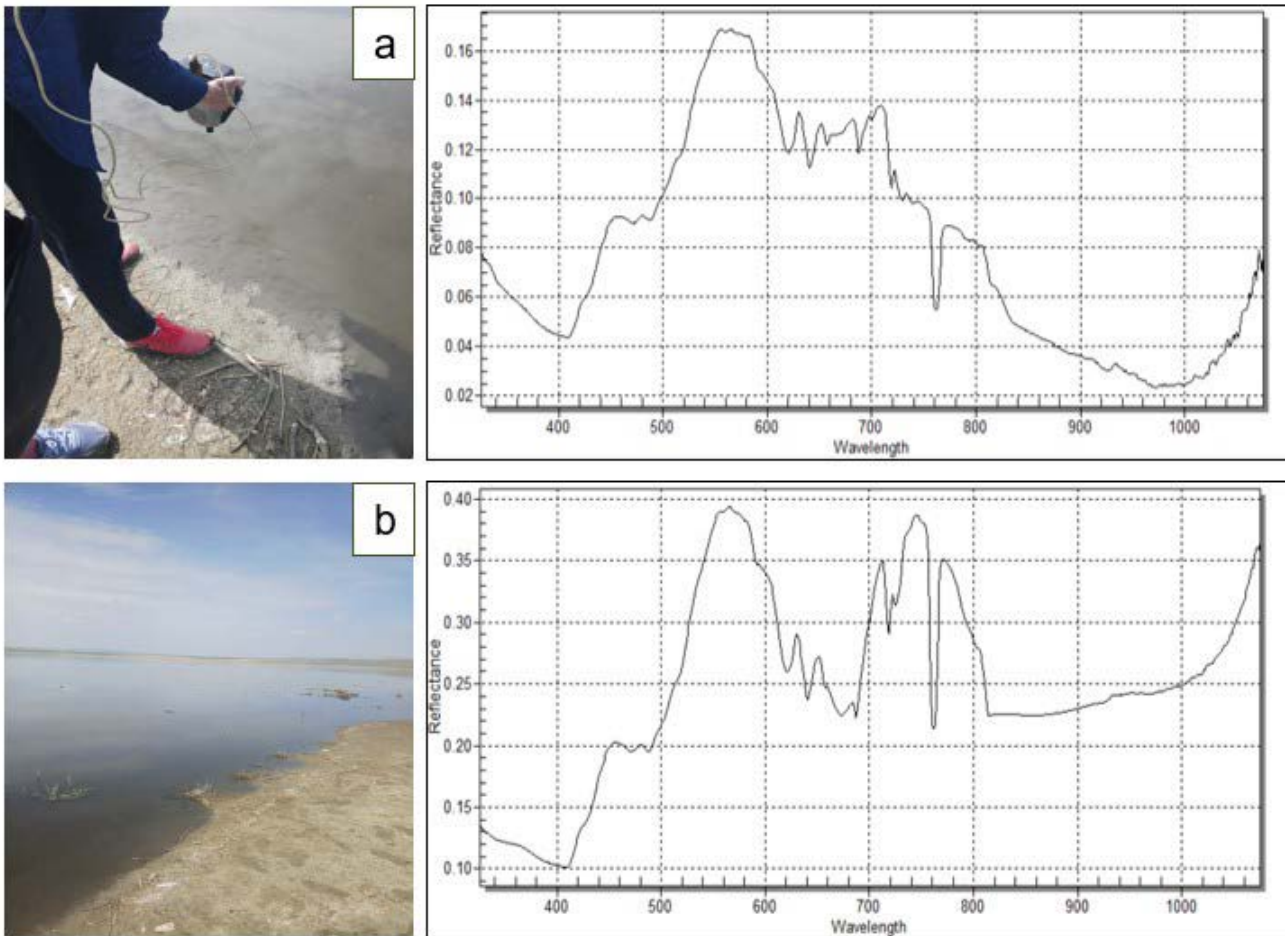


Fig. 4. Spectral signature of water (a) and wet soil (b).

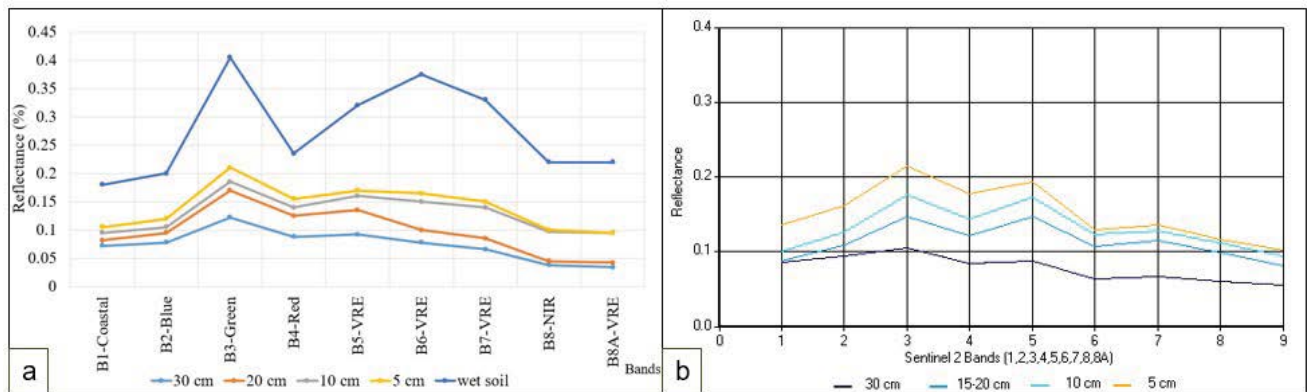


Fig. 5. (a) Average spectral reflectance of four water classes and wet soil and (b) reflectances of four water classes resampled to Sentinel-2 MSI image.



Fig. 6. Spectrometers and depth measurements locations.

algorithms were applied with two different training datasets to obtain the spectral-based bathymetry of the shallow wetland. Four ML algorithms were selected for deriving bathymetry: RF, SVM, MLC, and NN.

RF classifier is an ensemble classifier that generates multiple decision trees using a randomly selected set of training samples and variables [37]. RF is a more powerful extension of decision trees and overcomes the overfitting problem that is the main disadvantage of the decision tree classifier [38]. RF automatically creates decision trees using the training data of an objective variable (e.g., water depth) and predictor variables (e.g., pixel values of satellite images) and provides the mean of the outputs from the trees of the regression model. Thus, compared with simple empirical or semi-empirical other models, RF can create more accurate models based on real data [39].

Like RF, SVM and NN are also non-parametric supervised classifiers. The hyper-planes (support vectors) are selected in the SVM classification. These support vectors maximize the distance between the given classes [40].

This distance is called margin. Maximizing the margin provides data to separate the classes and decreases the probability of misclassification [38]. In the NN, there are processing nodes that are referred to as neurons. As a non-linear supervised classification algorithm, NN uses a standard backpropagation algorithm by choosing the number of hidden layers and activation function. It uses the weights of neurons interconnected with all neurons in the other layers, instead of the algorithm to regulate the network connection, and adjusts the weights in the nodes to minimize the error between the actual network output and the output for learning activity [41–43].

MLC is a parametric supervised classifier. It depends on the statistics of a Gaussian probability density function model for each class and computes the likelihood of unknown measurement based on the Bayesian equation [40,44]. Unlike the other algorithms, it is based on a clear statistical approach and has been widely selected for wetland classification.

### 3.3. Accuracy assessment

The main objective of the accuracy assessment is quantified accuracy of the produced classification maps by error matrix, also known as confusion matrix [45]. The obtained data were summarized in the error matrix. The main elements of the error matrix are producer's accuracy (PA), user's accuracy (UA), overall accuracy (OA), and kappa coefficient (K) [46]. Whereas PA defines the map producer's identification of the land cover types on the map from the satellite image, UA defines the land cover types on the ground by a person using the map. OA considers the diagonal elements of the error matrix and defines the similarity of the classified map from the land cover types on the ground [45].  $K$  is assessing the actual and chance agreements between the map and ground data, considering all elements in the confusion matrix [47,48].  $K$  values vary between 0 and 1, and the closer  $k$  approaches 1, the higher the accuracy. PA, UA, OA, and  $K$  parameters were calculated for each classification result via the following equations.

$$PA = \frac{\text{Samples correctly identified in the column}}{\text{Column total}} \times 100 \quad (1)$$

Table 2  
Confusion matrices of the classification algorithms with two datasets

	dataset1						dataset2						
SVM	Non-water	water1	water2	water3	water4	User Acc. (%)	SVM	Non-water	water1	water2	water3	water4	User Acc. (%)
Non-water	132,631	0	0	0	233	99.82	Non-water	132,306	0	0	0	98	99.93
water1	0	11,954	326	0	0	97.35	water1	11	12,488	567	11	0	95.50
water2	5	4,200	25,936	12,164	4	61.30	water2	49	3,666	25,334	2,930	120	78.92
water3	387	0	1,825	12,064	2,008	74.08	water3	5	0	2,042	19,883	590	88.29
water4	307	0	0	26	1,830	84.60	water4	959	0	144	1,430	3,267	56.33
Prod. Acc. (%)	99.48	74.00	92.34	49.74	44.91		Prod. Acc. (%)	99.23	77.31	90.20	81.98	80.17	
Over. Acc.	89.57%						Over. Acc.	93.87%					
Kappa	0.807						Kappa	0.887					
NN	Non-water	water1	water2	water3	water4	User Acc. (%)	NN	Non-water	water1	water2	water3	water4	User Acc. (%)
Non-water	132,971	0	0	0	1,033	99.23	Non-water	131,917	0	0	0	82	99.94
water1	0	14,134	9,403	0	0	60.05	water1	5	10,327	44	0	0	99.53
water2	0	1,910	12,508	1,559	0	78.29	water2	98	5,827	22,365	1,568	32	74.82
water3	359	110	6,176	22,695	3,042	70.09	water3	0	0	4,563	19,018	51	80.48
water4	0	0	0	0	0	0.00	water4	1,310	0	1,115	3,668	3,910	39.09
Prod. Acc. (%)	99.73	87.50	44.53	93.57	0.00		Prod. Acc. (%)	98.94	63.93	79.63	78.41	95.95	
Over. Acc.	88.54%						Over. Acc.	91.08%					
Kappa	0.788						Kappa	0.837					
ML	Non-water	water1	water2	water3	water4	User Acc. (%)	ML	Non-water	water1	water2	water3	water4	User Acc. (%)
Non-water	132,688	5,295	15,443	3,489	1,229	83.90	Non-water	132,723	161	398	581	1,204	98.26
water1	0	7,097	8	0	3	99.85	water1	0	8,040	158	0	0	98.07
water2	0	2,555	7,674	179	45	73.41	water2	1	7,841	22,801	4,549	65	64.67
water3	212	1,207	4,962	20,545	2,235	70.45	water3	0	75	3,018	14,979	12	82.83
water4	430	0	0	41	563	54.45	water4	606	37	1,712	4,145	2,794	30.06
Prod. Acc. (%)	99.52	43.93	27.32	84.71	13.82		Prod. Acc. (%)	99.54	49.77	81.18	61.76	68.56	
Over. Acc.	81.87%						Over. Acc.	88.07%					
Kappa	0.619						Kappa	0.778					
RF	Non-water	water1	water2	water3	water4	User Acc. (%)	RF	Non-water	water1	water2	water3	water4	User Acc. (%)
Non-water	132,836	0	0	0	623	99.53	Non-water	132,428	0	1	47	238	99.78
water1	0	11,407	8,279	9	0	57.92	water1	10	14,179	3,698	114	19	78.68
water2	85	4,121	6,614	464	25	58.48	water2	44	1,973	18,777	756	5	87.11
water3	205	626	13,194	23,732	1,834	59.94	water3	36	2	5,611	21,958	410	78.37
water4	204	0	0	49	1,593	86.29	water4	812	0	0	1,379	3,403	60.83
Prod. Acc. (%)	99.63	70.61	23.55	97.85	39.09		Prod. Acc. (%)	99.32	87.77	66.85	90.53	83.51	
Over. Acc.	85.57%						Over. Acc.	92.64%					
Kappa	0.734						Kappa	0.865					



Table 4  
Areal comparison of the ML classification results

Algorithm	Training data (Number of pixel)	water1 (ha)	water2 (ha)	water3 (ha)	water4 (ha)	Total water surface area (ha)
Reference map		161.54	280.87	242.54	40.06	725.01
NDWI						725.53
MLC	≥100	145.31	180.98	276.28	119.89	722.46
MLC	<100	71.08	104.53	291.61	10.34	477.56
SVM	≥100	161.47	268.93	240.93	69.83	741.16
SVM	<100	122.80	423.09	162.84	21.63	730.36
NN	≥100	260.01	143.40	262.18	76.25	741.84
NN	<100	235.37	159.77	323.82	0	718.96
RF	≥100	167.29	254.4	255.44	62.55	739.68
RF	<100	196.95	113.09	395.91	18.46	724.41

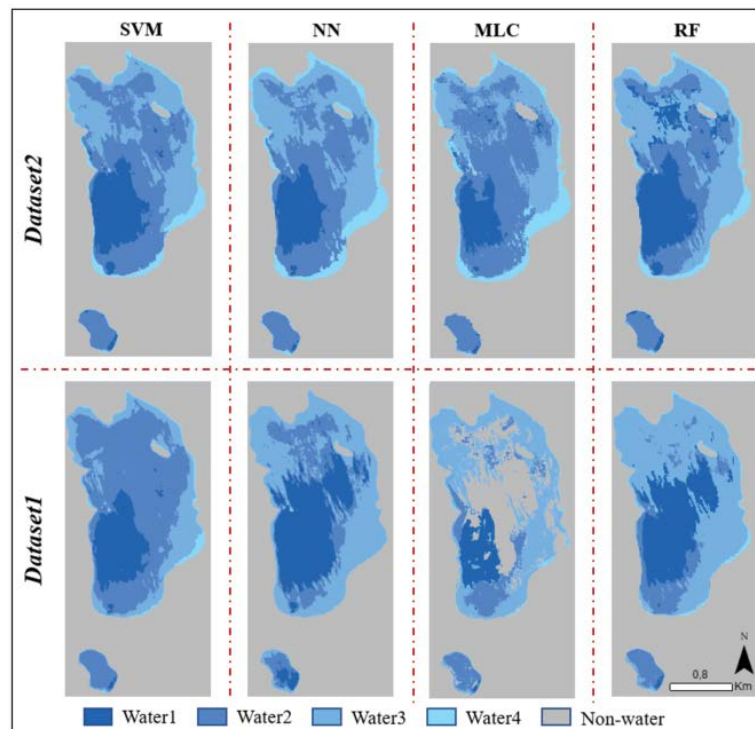


Fig. 7. Classification results: dataset1: number of pixels <100, dataset2: number of pixels ≥100.

value are obtained with RF (dataset1), MLC (dataset2), and SVM (dataset1), respectively. Besides, MLC (dataset1) gave the worst result, and insufficient training pixel number was thought to be a factor in this. It may be for the same reason that NN (dataset1) cannot classify all four classes. It has been observed that the MLC algorithm is more affected by the number of training datasets. The difference between classifications with dataset2 is lower comparing with classification with dataset1. Bathymetric maps obtained with two data sets and four classification methods are given in Fig. 7.

In Fig. 8, the NDWI results showing the total water surface area, the bathymetric reference map obtained with the spectral signatures, the RF (dataset2) result, which is

visually and as surface area closest to the reference; and SVM (dataset2), which gave the highest results in accuracy assessment, are given together.

## 5. Conclusion

The study demonstrated that remote sensing is an effective method for analyzing the wetlands, easily identified with the medium spatial resolution Sentinel-2 optical images.

This study indicated that ML classification algorithms could derive shallow water bathymetry with a spectral-based approach. According to the accuracy assessment,

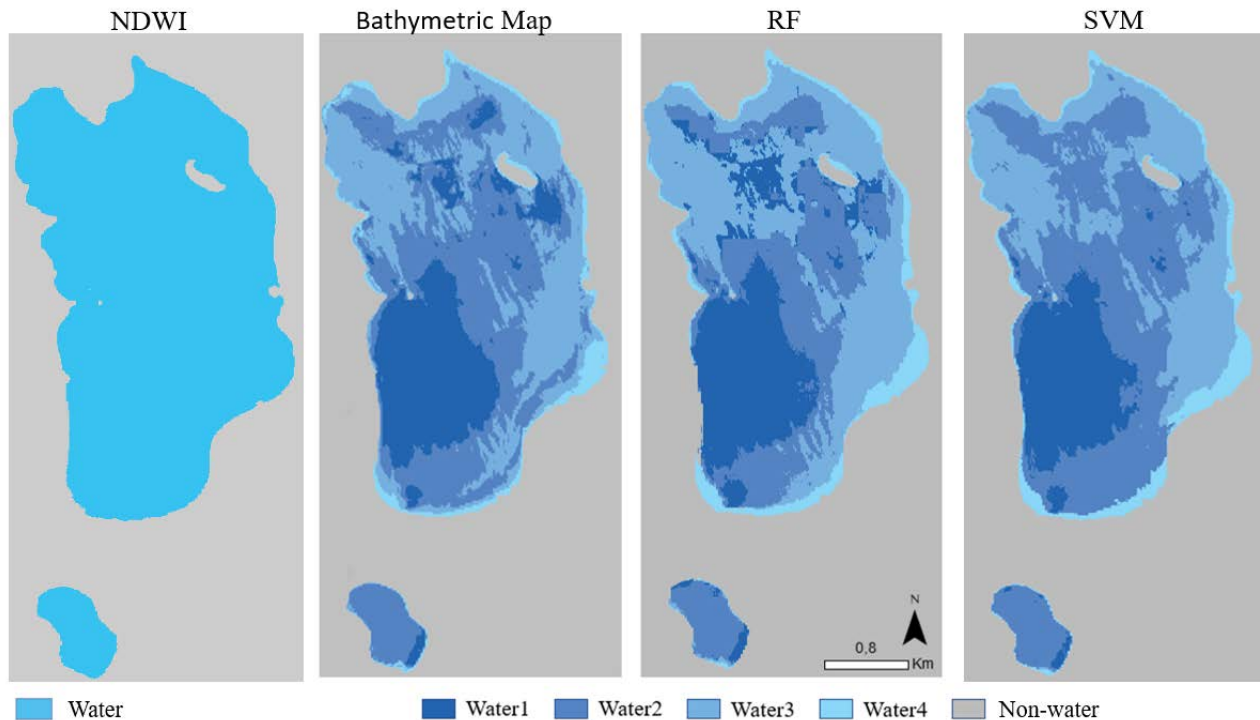


Fig. 8. NDWI, bathymetric map, RF and SVM classification (based on dataset2) results.

the SVM and RF method with dataset2 (number of pixels  $\geq 100$ ) showed almost close results and better performances than the others. On the other hand, low accuracies were obtained with dataset1 (number of pixels  $< 100$ ). At the same time, acceptable results were obtained with dataset2 in NN, and MLC algorithms, respectively. Low accuracies were obtained with dataset1 except for SVM and the worst performance was obtained in MLC with dataset1. When the areas of the four water classes determined by the four classification algorithms are compared, it is seen that the values are not very similar. According to the total water area, RF (dataset1) and MLC (dataset2) results are close to the total water area. However, SVM and RF classification results with dataset2 gave close values in class-based areal comparison. In addition, visual comparison of these two results resembled the bathymetry map created with ground truth data.

SVM and RF algorithms are seen to be powerful methods for classifying remotely sensed data, however, the best algorithm for a given task may be case-specific and may depend on the classes mapped, the nature of the training data, and the prediction variables provided. Therefore, users should experiment with multiple classifiers and training data to identify the best method.

The study was limited to a single period because the pandemic created a problem to reach the lake area. The results can be confirmed with studies to be repeated on different dates. In future studies, performances can be evaluated using high-resolution satellite images and other ML classification algorithms and also deep learning methods such as deep neural networks. Additionally, by testing this study in wetlands with bathymetric maps produced by the classical method, the accuracy of satellite-derived bathymetric maps can be investigated.

## References

- [1] L.M. Cowardin, V. Carter, F.C. Golet, E.T. LaRoe, Classification of Wetlands and Deepwater Habitats of the United States, US Department of the Interior, US Fish and Wildlife Service, Washington DC, USA, 1979.
- [2] Z. Liu, Z. Yao, R. Wang, Automatic identification of the lake area at Qinghai-Tibetan Plateau using remote sensing images, *Quat. Int.*, 503 (2019) 136–145.
- [3] R.J. Zomer, A. Trabucco, S.L. Ustin, Building spectral libraries for wetlands land cover classification and hyperspectral remote sensing, *J. Environ. Manage.*, 90 (2009) 2170–2177.
- [4] S. Khorram, F.H. Koch, C.F. van der Wiele, S.A. Nelson, Remote Sensing, Springer Science and Business Media, New York, USA, 2012.
- [5] C. Flener, E. Lotsari, P. Alho, J. Käyhkö, Comparison of empirical and theoretical remote sensing-based bathymetry models in river environments, *River Res. Appl.*, 28 (2012) 118–133.
- [6] E.C. Geyman, A.C. Maloof, A simple method for extracting water depth from multispectral satellite imagery in regions of variable bottom type, *Earth Space Sci.*, 6 (2019) 527–537.
- [7] W.D. Philpot, Bathymetric mapping with passive multispectral imagery, *Appl. Optics*, 28 (1989) 1569–1578.
- [8] V. Lafon, J.M. Froidefond, F.T. Lahet, P. Castaing, SPOT shallow water bathymetry of a moderately turbid tidal inlet based on field measurements, *Remote Sens. Environ.*, 81 (2002) 136–148.
- [9] J. Gao, Bathymetric mapping by means of remote sensing: methods, accuracy and limitations, *Prog. Phys. Geogr.*, 33 (2009) 103–116.
- [10] M. Amani, S. Mahdavi, O. Berard, Supervised wetland classification using high spatial resolution optical, SAR, and LiDAR imagery, *J. Appl. Remote Sens.*, 14 (2020) 024502, doi: 10.1117/1.JRS.14.024502.
- [11] J. Rogan, J. Franklin, D. Stow, J. Miller, C. Woodcock, D. Roberts, Mapping land-cover modifications over large areas: a comparison of machine learning algorithms, *Remote Sens. Environ.*, 112 (2008) 2272–2283.
- [12] G.H. Ball, D.J. Hall, ISODATA, A Novel Method of Data Analysis and Pattern Classification, Stanford Research Institute, Menlo Park CA, 1965.

- [13] Y. Zhong, L. Zhang, B. Huang, P. Li, An unsupervised artificial immune classifier for multi/hyperspectral remote sensing imagery, *IEEE Trans. Geosci. Remote Sens.*, 44 (2006) 420–431.
- [14] A.W. Abbas, N. Minallh, N. Ahmad, S.A.R. Abid, M.A.A. Khan, K-Means and ISODATA clustering algorithms for landcover classification using remote sensing, *Sindh Univ. Res. J.-SURJ (Science Series)*, 48 (2016) 315–318.
- [15] M.V. Herbei, F. Sala, M. Boldea, Using mathematical algorithms for classification of LANDSAT 8 satellite images, *AIP Conf. Proc.*, 1648 (2015) 670004, doi: 10.1063/1.4912899.
- [16] G. Camps-Valls, Machine Learning in Remote Sensing Data Processing, 2009 IEEE International Workshop on Machine Learning for Signal Processing, IEEE, Grenoble, France, 2009, pp. 1–6.
- [17] S. Tian, X. Zhang, J. Tian, Q. Sun, Random forest classification of wetland landcovers from multi-sensor data in the arid region of Xinjiang, China, *Remote Sens.*, 8 (2016) 954, doi: 10.3390/rs8110954.
- [18] M. Amani, B. Salehi, S. Mahdavi, J.E. Granger, B. Brisco, A. Hanson, Wetland classification using multi-source and multi-temporal optical remote sensing data in Newfoundland and Labrador, Canada, *Can. J. Remote Sens.*, 43 (2017) 360–373.
- [19] N. Yagmur, N. Musaoglu, G. Taskin, Detection of Shallow Water Area with Machine Learning Algorithms, *The International Archives of the Photogrammetry, Remote Sensing and Spatial Information Sciences*, Volume XLII-2/W13, 2019 ISPRS Geospatial Week 2019, 10–14 June 2019, Enschede, The Netherlands, 2019, pp. 1269–1273.
- [20] N. Wagle, T.D. Acharya, V. Kolluru, H. Huang, D.H. Lee, Multi-temporal land cover change mapping using google earth engine and ensemble learning methods, *Appl. Sci.*, 10 (2020) 8083, doi: 10.3390/app10228083.
- [21] T. Kiss, G. Sipos, Braid-scale channel geometry changes in a sand-bedded river: significance of low stages, *Geomorphology*, 84 (2007) 209–221.
- [22] J. Gao, Bathymetric mapping by means of remote sensing: methods, accuracy, and limitations, *Prog. Phys. Geogr.*, 33 (2009) 103–116.
- [23] S.D. Jawak, S.S.M. Vadlamani, A.J. Luis, A synoptic review on deriving bathymetry information using remote sensing technologies: models, methods and comparisons, *Adv. Remote Sens.*, 4 (2015) 147–162.
- [24] T. Lillesand, W. Ralph, R.W. Kiefer, J. Jonathan Chipman, *Remote Sensing and Image Interpretation*, 7th ed., Wiley, New York, USA, 2015.
- [25] J.M. Kerr, S. Purkis, An algorithm for optically-deriving water depth from multispectral imagery in coral reef landscapes in the absence of ground-truth data, *Remote Sens. Environ.*, 210 (2018) 307–324.
- [26] B. Ai, Z. Wen, Z. Wang, R. Wang, D. Su, C. Li, F. Yang, Convolutional neural network to retrieve water depth in marine shallow water area from remote sensing images, *IEEE J. Sel. Top. Appl. Earth Obs. Remote Sens.*, 13 (2020) 2888–2898.
- [27] <https://tvk.csb.gov.tr/konya-kulu-duden-golu-tescil-ilaniduyuru-406332>
- [28] <https://www.hurriyet.com.tr/gundem/180-kus-turune-ev-sahipligi-yapan-duden-golu-kurumaya-yuz-tuttu-41503568>
- [29] <https://anadoludabugun.com.tr/konya-haber/duden-golunun-su-seviyesindeki-dusus-tedirgin-ediyor-137559h>
- [30] [http://www.kop.gov.tr/pdf/KOP\\_Bolge\\_si\\_alanlar\\_raporu.pdf](http://www.kop.gov.tr/pdf/KOP_Bolge_si_alanlar_raporu.pdf)
- [31] <https://sentinel.esa.int/web/sentinel/user-guides/sentinel-2-msi>
- [32] D.R. Lyzenga, Passive remote sensing techniques for mapping water depth and bottom features, *Appl. Optics*, 17 (1998) 379–383.
- [33] C.D. Mobley, *Light and Water: Radiative Transfer in Natural Waters*, Academic Press, San Diego, 1994.
- [34] L. Hubert-Moy, A. Cottonne, L. Le Du, A. Chardin, P. Perez, A comparison of parametric classification procedures of remotely sensed data applied on different landscape units, *Remote Sens. Environ.*, 75 (2001) 174–187.
- [35] D.A. Landgrebe, *Signal Theory Methods in Multispectral Remote Sensing*, John Wiley and Sons, New Jersey, USA, 2003.
- [36] P.M. Mather, M. Koch, *Computer Processing of Remotely-Sensed Images: An Introduction*, 3rd ed., John Wiley and Sons, New Jersey, USA, 2011.
- [37] M. Belgiu, L. Drăguț, Random forest in remote sensing: a review of applications and future directions, *ISPRS ISPRS J. Photogramm. Remote Sens.*, 114 (2016) 24–31.
- [38] T.V. Bijeesh, K.N. Narasimhamurthy, Surface water detection and delineation using remote sensing images: a review of methods and algorithms, *Sustainable Water Res. Manage.*, 6 (2020) 1–23.
- [39] M.D.M. Manessa, A. Kanno, M. Sekine, M. Haidar, K. Yamamoto, T. Imai, T. Higuchi, Satellite-derived bathymetry using random forest algorithm and worldview-2 imagery, *Geoplanning J. Geomatics Plann.*, 3 (2016) 117–126.
- [40] J.R. Otukei, T. Blaschke, Land cover change assessment using decision trees, support vector machines and maximum likelihood classification algorithms, *Int. J. Appl. Earth Obs. Geoinf.*, 12 (2010) 27–31.
- [41] X. Jiang, M. Lin, J. Zhao, Woodland Cover Change Assessment Using Decision Trees, Support Vector Machines and Artificial Neural Networks Classification Algorithms, 2011 Fourth International Conference on Intelligent Computation Technology and Automation, IEEE, 2011, pp. 312–315.
- [42] J.A. Richards, *Remote Sensing Digital Image Analysis*, Springer-Verlag, Berlin, 1999.
- [43] C.D. Schuman, J.D. Birdwell, Dynamic artificial neural networks with affective systems, *PLoS One*, 8 (2013) e80455, doi: 10.1371/journal.pone.0080455.
- [44] J.D. Paola, R.A. Schowengerdt, A detailed comparison of backpropagation neural network and maximum-likelihood classifiers for urban land use classification, *IEEE Trans. Geosci. Remote Sens.*, 33 (1995) 981–996.
- [45] G.M. Foody, Status of land cover classification accuracy assessment, *Remote Sens. Environ.*, 80 (2002) 185–201.
- [46] D. Lu, Q. Weng, A survey of image classification methods and techniques for improving classification performance, *Int. J. Remote Sens.*, 28 (2007) 823–870.
- [47] R.G. Congalton, Accuracy assessment and validation of remotely sensed and other spatial information, *Int. J. Wildland Fire*, 10 (2001) 321–328.
- [48] G.H. Rosenfield, K. Fitzpatrick-Lins, A coefficient of agreement as a measure of thematic classification accuracy, *Photogramm. Eng. Remote Sens.*, 52 (1986) 223–227.
- [49] Y. Qian, W. Zhou, J. Yan, W. Li, L. Han, Comparing machine learning classifiers for object-based land cover classification using very high resolution imagery, *Remote Sens.*, 7 (2014) 153–168.
- [50] C. Huang, L.S. Davis, J.R.G. Townshend, An assessment of support vector machines for land cover classification, *Int. J. Remote Sens.*, 23 (2002) 725–749.
- [51] S.K. McFeeters, The use of the Normalized Difference Water Index (NDWI) in the delineation of open water features, *Int. J. Remote Sens.*, 17 (1996) 1425–1432.